MASTER THESIS

THE EFFECT OF PERTURBING THE ANGULAR MOMENTUM DURING WALKING ON THE BALANCE STRATEGY

Jolien I. Ambrosius

FACULTY OF ENGINEERING TECHNOLOGY
DEPARTMENT OF BIOMECHANICAL ENGINEERING

EXAMINATION COMMITTEE
M. van Mierlo Msc.
Dr. E.H.F. van Asseldonk
Prof.dr. J.H. Buurke

DOCUMENT NUMBER
BE - 814

UNIVERSITY OF TWENTE.

21-10-2021

The effect of perturbing the angular momentum during walking on the balance strategy

Jolien I. Ambrosius
Master Thesis Biomechanical Engineering
Department of Biomechanical Engineering, University of Twente, Enschede, The Netherlands

October 2021

***Abstract* - In the development of exoskeletons, balance control during walking is an important factor. Humans solve disbalance due to external perturbations during walking using the hip, ankle and/or stepping strategy. Although, no studies have been performed analyzing the used balance strategies after perturbing solely the angular momentum. This study performed experiments with 10 subjects. Each subject walked on a treadmill (with normal and slow (typical exoskeleton) walking speed) and received perturbations in the anterior and posterior (AP) direction on the upper body and simultaneously in opposite direction on the pelvis at toe-off right (TOR). Motion and force plate data were obtained to investigate the balance recovery strategy. The combination of the two perturbations resulted in a minimal change in the linear momentum and an affected angular momentum. We analysed the balance strategy in the first half gait cycle after perturbation. We looked into the moment arm which is calculated using the GRF and CoP-CoM distance. We found that the moment arm did not absolute linearly increase after increasing forward or backward perturbations. However, the GRF in AP direction did show at the end of the perturbation a significant effect after increasing forward ($p<0.001$) and backward ($p=0.002$) perturbation magnitudes, during both walking speeds. This resulted in a response to the affected angular momentum during the perturbation, by creating an angular momentum in opposite direction. Finally, CoP-CoM distance in AP direction was minimally affected due to the minimal affected linear momentum. The analysed balance strategies may contribute to a better human-like controller for the exoskeleton.**

1 Introduction

The human body has a constant focus on maintaining balance. A walking movement results in a constant falling motion, and recovery therefrom. Besides walking, the human also needs to respond to external perturbations in order to remain in balance. This response is very complex and involves for example muscles and joints. In the past years, multiple studies have investigated the balance recovery of humans with or without perturbations in mediolateral and anteroposterior directions both during gait and standing [1], [2], [3]. These studies gave more insight into human balance strategies, which is useful for the development of the balance control of an exoskeleton which helps humans who have difficulty with walking.

It is important to maintain balance during walking and other activities involving movement. While standing still, the goal is to keep the Center of Mass (CoM) in the base of support (BoS)[1]. However, the CoM velocity also plays an important role in maintaining balance during walking. Hof et al. introduced the extrapolated center of mass (XCoM) concept [4]. The XCoM is a combination of the CoM position (projected on the ground) and the CoM velocity and shows a model to achieve stable walking. Stable walking means no falling, no increasing of fluctuating walking speed, no change in step length and the walker follows a well-defined course. It has been shown that when someone places his foot at the position of the XCoM, they come to a halt. However, when the foot is placed behind and outward of the position of the XCoM, stable walking is observed. Although, disturbances may affect the CoM velocity. This can be solved by changing the foot to the direction of the disturbances. [4] [5]

Balance during walking or while standing is maintained using balance recovery strategies.

They can be distinguished in the ankle, hip and stepping strategy (Figure 1). The Center of Pressure (CoP) is a representation of the point of application of the Ground Reaction Force (GRF). The GRF is the external force exerted by the ground on the human body. In the ankle strategy, an ankle torque is generated which results in a change of the GRF and its location (CoP), this regulates the CoM motion. When the perturbation is larger, the hip strategy is necessary to maintain balance. A hip torque is generated which creates a moment around the CoM causing adaptation in the GRF. When the hip and ankle strategy are insufficient to recover from disbalance, the stepping strategy enlarges the Base of Support (BoS) by taking a step. [6], [7]

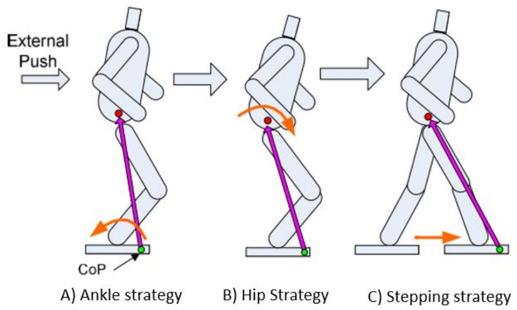

Figure 1: **Balance strategies.** A) Ankle strategy B) Hip strategy C) Stepping strategy [6]

Multiple studies focused on the balance recovery of humans. Rietdyk et al. studied the balance recovery after mediolateral (ML) perturbations on the upper body during standing, and found that the hip and spinal moment are the most involved in moving the CoP during the recovery (85 %) whereas the ankles are less involved (15 %). [1]. M. van den Bogaart et al. applied anteroposterior (AP) perturbations during treadmill walking by accelerating the treadmill speed to provide a slip effect and focused on the behaviour of the CoM. They found that the stepping and ankle strategy contributed to a change in the CoM acceleration after perturbation. The counter-rotation mechanism (changing the angular momentum with GRF) did counteract the caused CoM acceleration after perturbation, which prevented interference of the gait pattern. [2]. Madehkhaksar et al. found that the participants walked with a shorter stride length, a wider step width and a higher cadence after anteroposterior and mediolateral perturbations, which all increased the Margin of Stability (the distance from the leading toe to the XCoM). These findings (wider step, shorter stride length and higher cadence) help to restore the balance during walking. However, the effects of the ML perturbations were much greater compared to the AP perturbations, which indicates a greater instability in the ML direction. [8] Sheehan Et al. perturbed patients with a leg amputation and focused on the angular momentum. They observed that angular momentum ranges were smaller for patients with a prosthetic leg compared to patients with a intact leg. However, the patients with amputation were more destabilized by perturbations during walking than healthy patients which they solved by altering motion of the intact limbs. [9]

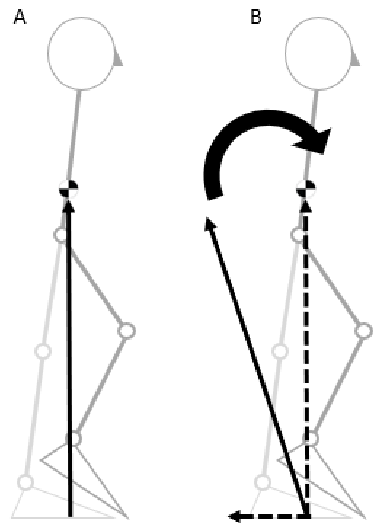

Figure 2: **The impact of the GRF on the CoM (gray circle)**. a) The GRF (solid arrow) goes through the CoM, what results in no angular momentum. b) The GRF is directed backward from CoM, which causes an increase of the angular momentum in forward direction. GRF is split into a horizontal and a vertical component (dotted arrow). [10]

Looking at the balance reaction of the human body, we observe that the GRF is an important factor. During a perturbation, the linear and angular momentum are affected due to changing GRF magnitude and direction. In order to resolve these changed momenta, an AP directed GRF in opposite direction than during the perturbation is created. This method is called the counter-rotation mechanism and prevents mainly the interference with the gait pattern. An adapted AP GRF directed backwards of the CoM creates a forward angular impulse, which changes the angular momentum about the CoM, as shown in Figure 2. [11] Besides the horizontal GRF, the vertical and ML GRF also influence the magnitude and direction of the created angular momentum. [2]

Humans degrade their walking speed to improve their stability.[12] Wu et al. investigated the gait mechanics during slow walking. First, they observed that GRFs in AP, ML and vertical direction decrease over the gait cycle during slower walking speed. Secondly, the total joint power also decreases over the gait cycle. Lastly, they found that the angle, moment and power of the ankle, knee and hip joints diminish in slower walking speeds. [13]

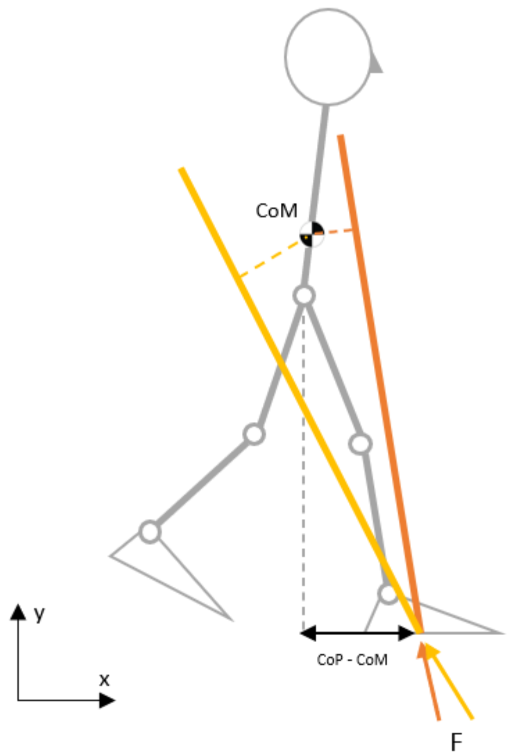

Figure 3: **Moment arm of the GRF with respect to the CoM**. The yellow and orange dotted line represents the moment arm. The negative moment arm (yellow dotted) result in a forward angular momentum and the positive moment arm (orange dotted line) result in backward angular impulse.

The above-mentioned studies performed experiments perturbing the angular and linear momentum or only linear momentum. However, the effect of perturbing the angular momentum on the balance recovery is still unknown. This study investigated the balance strategy after perturbing the angular momentum whilst minimizing the effects on the linear momentum during walking. To focus on the angular momentum, it is necessary to minimize the linear momentum. Our results present the balance recovery after perturbing the angular momentum during slow (corresponding to the walking speed using an exoskeleton) and normal walking speeds. Both speeds have been investigated since it has been shown that the normal walking speed is more stable compared to the slow walking speed [14] which are caused by changing gait mechanics [13]. We focused on the balance strategy in the first gait cycle after perturbation. Within the balance strategy, we started with quantifying the moment arm (relative to CoM). This moment arm quantifies the magnitude and direction of the GRF. Since the direction and magnitude of the GRF and of the CoP-CoM distance (in AP direction) influence the moment arm, they will be analysed afterwards (see Figure 3). The CoP-CoM distance in AP direction is in linear relation with the horizontal CoM velocity. [3] According to this relation, we expect that the CoP-CoM distance will be minimally affected by the perturbation, since minimal affected linear momentum implies minimal affected horizontal CoMv. If the angular momentum is affected due to perturbation, the GRF in AP direction adapt during and also after perturbation to maintain balance. This AP GRF is in opposite direction compared to the GRF during the perturbation, to solve the disbalance. Due to the affected AP GRF, we finally expect a change in the moment arm.

2 Materials & Method

2.1 Participants

Ten healthy participants with no known history of neurological muscular or orthopaedic problems participated in this study (6 women, 4 men, age 24.4 ± 3.5 year, weight 66.3 ± 6.9 kg, height 1.75 ± 0.06 meter, means ± s.d.). The experiment protocol was approved by the local ethics committee of the University of Twente. All subjects gave prior informed consent.

2.2 Materials

Subjects walked on a dual-belt treadmill (custom Y- Mill, Motekforce Link, Culemborg, The Netherlands) during the experiment. Under each belt, a force plate was placed to measure 3 degrees-of-freedom GRFs and moments. Perturbations were applied with two motors (SMH60, Moog, Nieuw-Vennep, The Netherlands) located at the rear side of the treadmill, one to apply perturbations on the pelvis and one on the upper body level (at the top of the thoracic vertebrae), see Figure 4. The two motors (with a maximum deflection of 1.1 in anterior and posterior direction) were mounted onto separated steel support structures next to the treadmill to ensure it did not influence the force plates. Each motor had a carbon lever arm (0.3 m) attached to a rotational axis, consisting of a load cell (model QLA131, FUTEK, Los Angeles, CA, USA) to measure the force. A carbon rod was attached at the end of each lever arm with a ball joint. The upper rod (0.9 m in length) was fixed to the rear side of the upper body brace, which is an adapted commercially available body protector (Bodyprotector USG Flexi). The pelvis rod (1.1 m in length) was fixed to the rear side of the modified universal pelvis abduction brace (Distrac Wellcare, Hoegaarden, Belgium). Both rods were horizontal when the pelvis and upper body brace were worn by the subject. See Figure 4 for the schematic overview of the setup.

Motor control signals were generated at 1000 Hz using xPC-target (MathWorks, Natick, MA, USA) and sent to the motor drivers over ethernet (User Datagram Protocol), with a dedicated ethernet card (82558 ethernet card, Intel, Santa Clara, CA, USA). The same xPC-target was used to collect 3 degrees-of-freedom ground reaction forces and moments of each of the two force plates in the treadmill, using a PCI-6229 AD card (National Instruments, Austin, TX, USA). The perturbations are controlled by the Testmanager (Ingenieurgemeinschaft IgH, 2000-today) in real time. In this controller, the perturbation magnitudes were adapted to the weight of the subjects (see Table 1) and a calculation for giving the perturbation at the right time within the gait phase has been performed.

2.3 Data collection

Kinematic data were collected using an infrared camera motion capture system (Qualisys Motion Capture system series 6+) and recorded by Qualisys track manager (QTM) at a frequency of 128 Hz. Reflective markers were used to measure the motion with the cameras. The load cell force-, perturbation-, motor torque- and encode angle -data were acquired at 1000 Hz using ethernet cables. Analog data measured by the force plates in the treadmill was recorded with a Qualysis analog interface at 2048 Hz. The xPC target software is used to generate an analog signal for synchronization with the motion capture system.

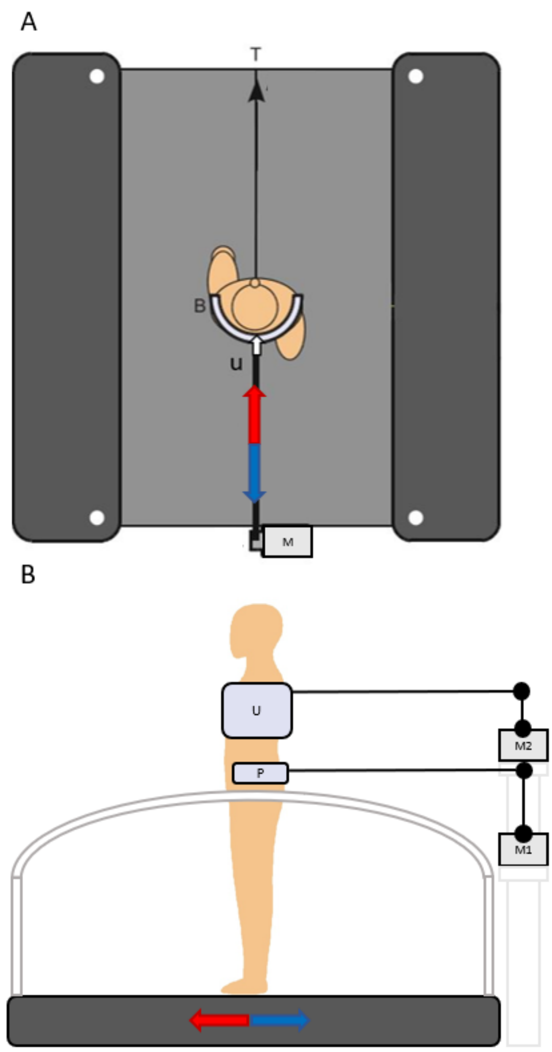

Figure 4: **Schematic overview of the experiment setup.** A: Top view. B: Side view. The motors are placed to the rear side of the treadmill. P: pelvis perturbation location. U: upper body perturbation location. M: Motor 1 (pelvis) and motor 2 (upper body). Red arrow relates to the positive perturbations and the blue arrow the negative perturbations. T: Treadmill.

2.4 Experimental protocol

Prior to starting the experiment, reflective markers (single and clusters) were attached to the subject. Single markers were attached to the following anatomical positions repeated for left and right body side: first and fifth metatarsus, calcaneus, medial and lateral malleoli, medial and lateral femur epicondyle, anterior and posterior iliac spine, medial and lateral humeral epicondyle, ulnar and radial styloid, second and fifth knuckle and acromion. Single markers are also placed on the cervical vertebra (C7) and on the posterior locations of the pelvis and upper body perturbations. Cluster markers (consisting of four single markers) are attached on the shank, thigh, upper arm and forearm for both left and right body sides. The last two cluster markers are placed on the anterior side of the sternum and pelvis. After the markers were applied, the subject was strapped into a safety harness (Honor, FBH-10) and the pelvis and upper body braces.

At the beginning of the experiment, static trials (standing still) were performed with and without the braces. The walking trials were performed at two different walking speeds: normal and slow (corresponding to exoskeleton) walking speed. The right walking speed for each subject was measured with the following formulae: $0.63\sqrt{l}\ m/s$ (slow speed) and $1.25\sqrt{l}\ m/s$ (normal speed) [15], where l is the leg length of the subject. The subjects were able to move their arms freely, as usually observed during walking. The measured trials and corresponding perturbation magnitudes are shown in table 1. Each trial consisted of 8 different perturbation magnitudes. Each perturbation magnitude was repeated 6 times, therefore resulting in a total number of 48 perturbations per trial. The perturbations were applied at toe-off right (TOR, see Figure 6) randomly between the 6-12 s during gait. The order of the trials differed between the subjects to avoid the contribution of fatigue in any of the trials. The coordinate system used during the experiments and the gait phases is shown in Figure 6.

2.5 Data processing

Marker data was measured with the Qualysis Track Manager (Version 2020.2). Afterwards, this data was imported in MATLAB (R2020a, MathWorks). The marker and force data were filtered with a 20 Hz low pass Butterworth filter. The motor and Qualysis data were synchronized using an analog synchronisation signal. The Qualysis motion data was added in OpenSim (4.1, Simbios) for scaling a generic musculoskeletal model to the subjects. After scaling, the inverse kinematic tool from OpenSim was used to calculate joint angles and the CoM position. In addition, the analyze tool in OpenSim was used to calculate CoM velocity, CoM acceleration, angular orientation, angular velocity and acceleration of the body segments. The Whole Body Angular Momentum (WBAM) is obtained with the formula given by Herr et al.:

$$\overrightarrow{WBAM} = \sum_{i=1}^{22}[\overrightarrow{r}^i_{CoM} - \overrightarrow{r}_{CoM} \times m_i(\overrightarrow{v}^i - \overrightarrow{v}_{CoM}) + \overset{\leftrightarrow}{I}^i \overrightarrow{\omega}^i][16] \quad (1)$$

The WBAM is calculated, by equation 1, as the sum of the angular momentum around the CoM of each body segment (using 22 segments). The $\overrightarrow{r}_{CoM}$ is the position of the CoM and $\overrightarrow{v}_{CoM}$ is the CoM velocity of the total body. $\overrightarrow{r}^i_{CoM}$ and $\overrightarrow{v}^i$ represent the CoM position and CoM velocity, respectively, for each segment. m_i is the mass of the corresponding segment and the $\overset{\leftrightarrow}{I}^i$ and $\overrightarrow{\omega}^i$ are the inertia tensor and angular velocity about the segments CoM, respectively. [16]

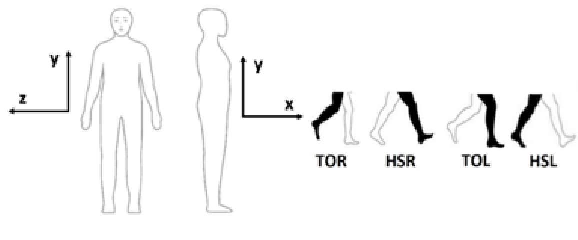

Figure 6: The used coordinate system and abbreviation for moments within one gait cycle. TOR = Toe of right, HSR = Heel strike right, TOL = Toe of left, HSL, Heel strike left

Table 1: **Experiment trials**. Negative magnitudes corresponds to backward perturbations and positive magnitudes to forward perturbations. The magnitude of the perturbation is a percentage of the body weight. Trials 101-102 are performed with normal walking speed and trials 103-104 with slow walking speed.

Trial	**Pelvis magnitude (%)**	**Upper body magnitude (%)**
101	0	0
102	[-4, -8, -12, -16, 4, 8, 12, 16]	= -pelvis
103	0	0
104	[-4, -8, -12, -16, 4, 8, 12, 16]	= -pelvis

2.6 Data analysis

The collected data were analysed in two steps. First, we looked at the effect of the perturbations on the linear and angular momentum, using the variables CoMv and WBAM over the entire gait cycle. In the second step, the balance strategy was investigated with an analysis of the moment arm, GRF and CoP-CoM distance. The moment arm with respect to the CoM illustrates the generated moment by the GRF (in sagittal plane). The moment arm is obtained by taking a line through the CoM and perpendicular to the GRF vector (as seen in Figure 3). For this calculation, we used the GRF in AP and vertical direction and the distance from CoP to CoM in AP direction. See Figure 3 for clarity over the calculated moment arm. After analysing the moment arm, we looked into the GRF and CoP-CoM distance, both in AP direction. All three variables were analysed at three moments within the first half gait cycle: EndP (end of the perturbation), Mid (between EndP and HSR) and HSR. The following abbreviations are used in the analysis: MA-EndP, MA-Mid, MA-HSR, CC-EndP, CC-Mid, CC-HSR, GRF-EndP, GRF-Mid, GRF-HSR. Boxplots are generated for the moment arm and GRF at each moment to show the measured distribution. The CoP-CoM distance is graphed in the transverse plane, using the distances in AP and ML direction.

2.7 Statistical analysis

The statistical analysis was performed with the use of a linear mixed model. To test the effect of the perturbation, we investigated if there is a linear relationship between the variables and the perturbation magnitude. To test linearity, the perturbation magnitudes are selected as covariate. Before adding the perturbation magnitudes as covariate, we separated the perturbations in four negative and four positive perturbations. The following variables were tested one by one in the linear mixed model: the moment arm, the GRF in AP direction and the CoP-CoM distance in AP direction. We took the mean of all measurements from each variable at three moments: EndP, Mid and HSR. First, the fixed effect model was built using the perturbation magnitude. Second, the random effect with including intercept was added for the previous mentioned fixed effect (perturbation magnitude), to allow variation between subjects. The statistical effect is calculated, separately, for normal and slow walking speed. We speak of statistical significance at the value $p < 0.05$. SPSS statistics 27 (IBM Corporation, Armonk, NY, USA) was used for the statistical analysis.

3 Results

The results are separated into two sections: the validation of the experiment and the balance recovery strategy. In the first section, the effect of applying upper body and opposite pelvis perturbations on the angular and linear momentum are observed. Thereafter, we focus on the balance recovery strategy after the applied perturbations.

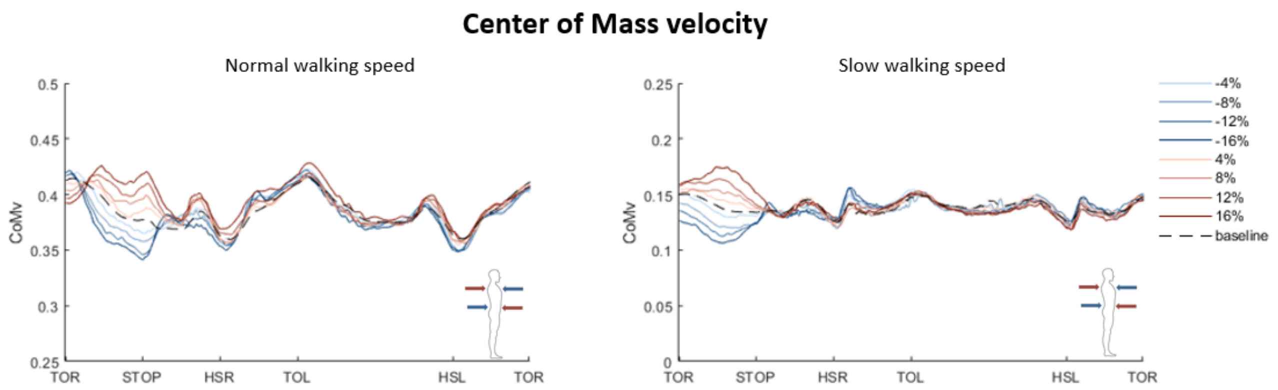

Figure 5: **Center of Mass velocity in x direction at two different walking speeds.** Data is plotted for the first gait cycle after perturbation. EndP represents the end of the perturbation. The perturbations magnitudes are shown in the legend as percentage of body mass. Positive (forward) perturbations corresponds to positive upper body and negative pelvis perturbations, vice versa for negative (backward) perturbations.

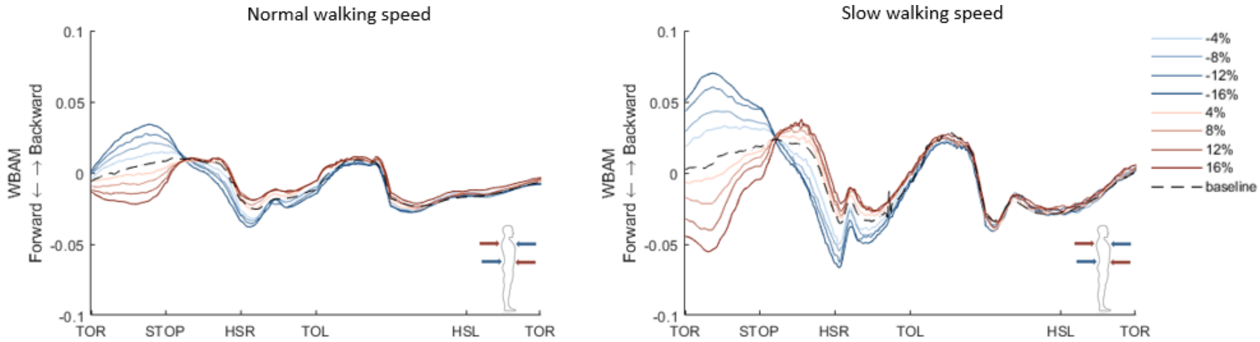

Figure 7: **Whole Body Angular Momentum around z-axis at two different walking speeds.** Plotted data of the first gait cycle after perturbation. EndP represents the end of the perturbation. The perturbations magnitudes are shown in the legend as percentage of body mass. The perturbations magnitudes are shown in the legend as percentage of body mass. Positive (forward) perturbations corresponds to positive upper body and negative pelvis perturbations, vice versa for negative (backward) perturbations.

3.1 Validation of the experiment

In the experiment, we applied the two opposite perturbations during walking to achieve a minimal linear momentum change. To validate this, the center of mass velocity (CoMv) is observed. Thereafter, the whole-body angular momentum is analysed to verify the effect of the perturbations.

3.1.1 Linear momentum

The perturbations minimally affect the CoMv. The amount of change in the CoMv depends on the perturbation magnitude, which can be observed in Figure 5. The CoMv is affected mostly during the perturbation (from TOR to EndP). In this phase, we see an increase in CoMv during forward perturbations and a decrease in CoMv during backward perturbations. For both perturbation directions applies: the greater the magnitude of the perturbation, the greater the CoMv change. In the normal walking speed graph, we see during backward perturbations a strong descent to a smaller CoMv. At the same moment, the CoMv of the forward perturbations increases but to a lesser extent compared to the backward perturbations. While, the CoMv change after forward and backward perturbations during slow walking are more equal. Both walking speeds resolve the change of CoMv within the gait cycle (the baseline CoMv is reached) but the reaction of the perturbation from TOR to HSR differs. In addition, the normal walking speed fluctuates, in general, more over the total gait cycle compared to the slow walking speed.

3.1.2 Angular momentum

The perturbations cause a change in WBAM directed backwards or forward, depending on perturbation direction. It is visible that the WBAM is mainly affected by the perturbation from TOR (start of perturbation) to TOL, as shown in FIgure 7. Backward perturbations result in backward angular momentum and forward perturbations result in forward angular momentum during the perturbation. However, this reverses short after the perturbations. The backward perturbations cause a forward angular momentum while the forward perturbations cause a backward angular momentum. Just like what happened at the CoMv: the greater the perturbation magnitude, the greater the change in WBAM. In general, the slow walking speed graph shows a marked greater change in the WBAM concerning the perturbation magnitudes when compared to that of the normal walking speed. Also, the flow of the WBAM baseline data during slow walking speed fluctuates more compared to normal walking speed baseline data. For both speeds, we observe that the change in WBAM is mostly solved at TOL.

3.2 Balance recovery strategy

In this, second, section we analyse the balance recovery strategy after perturbing the angular momentum at the two walking speeds. We saw in the previous section (Validation of the experiment) that the perturbation affects the balance mainly in the first half of the gait cycle (from TOR to TOL). After observing this, we will focus on the balance strategy only on this part of the gait cycle. Therefore, the results are pre-

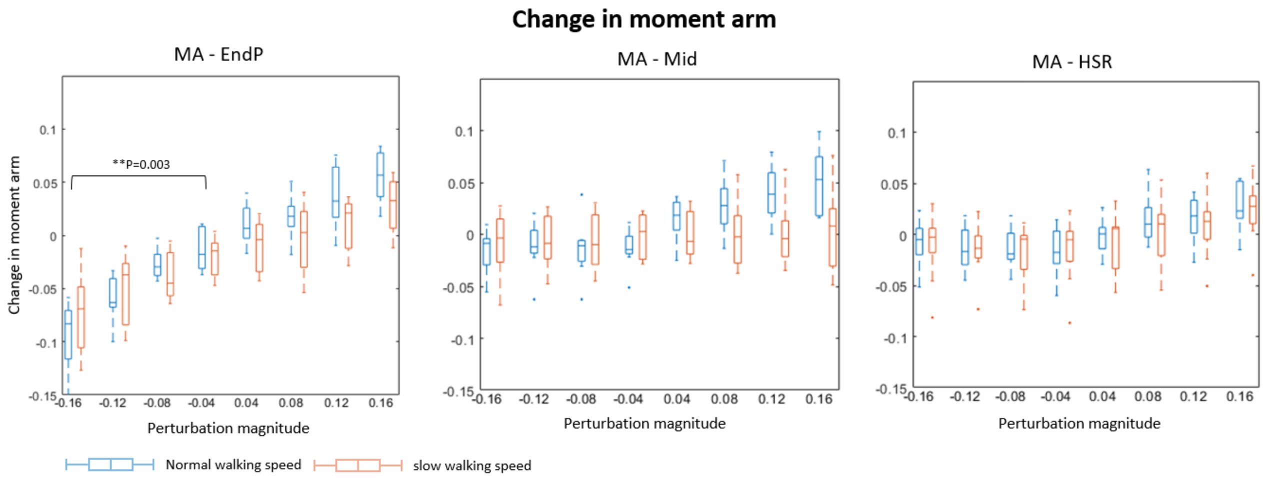

Figure 8: **Change in moment arm at EndP, between EndP and HSR (called 'Mid') and HSR**. The horizontal line in the boxplot represents the median, the top edge of the box represents the 75th percentile and the bottom of the box the 25th percentile. The vertical lines give an indication of the maximum and minimum value and the dots below and under the boxplots represent outliers. The baseline value at the specific moment within the gait cycle is subtracted from the perturbation data. The y-axis is normalized (using $\sqrt{\text{leg length}}$) and the x-axis represents the perturbation magnitude. The p-value is shown for moment arms which are significant affected by perturbation magnitude. A double asterisk (**) represent the statistics for slow walking speed. Baseline moment arm lengths: EndP 0.11 (normal) and 0.13 (slow), Mid 0.17 (normal) and 0.15 (slow) and HSR 0.28 (normal) and 0.19 (slow).

sented at the following three moments: EndP, Mid (between EndP and HSR) and HSR. First, we will look at the moment arm. Thereafter, the GRF and CoP-CoM distance, both in AP direction, are visualised to give more insight into the balance strategy.

3.2.1 Moment arm

No statistically significant linear relationship ($p<0.05$) between moment arm and perturbation magnitude is found for both perturbation directions in the three moments. One exception occurs at MA-EndP ($p=0.003$) for slow walking (statistical analysis results can be found in Appendix 5.2). However, the moment arm changes due to perturbations in the three moments, observe Figure 8. A increase or decrease is visible in the MA-EndP in both perturbation directions and for both speeds. Still, due to overlapping values, no significance is found. At MA-Mid, we observe that the moment arm after backward perturbations are almost equal to the baseline moment arm. On the other hand, the forward perturbations still affect MA-Mid at this moment for normal walking speed, but this is again not significant due to great variability. MA-Mid after forward perturbations during slow walking speed seems not affected, but the variability is high. The MA-Mid and MA-HSR both show no observable change after backward perturbations. MA-HSR is increased more when compared to MA-Mid after positive perturbations during slow walking, which is odd. The forward perturbations during normal walking speed have a lasting effect on the moment arm compared to backward perturbations. Observe in Appendix Section 5.1 Figure 12 the moment arm over the entire gait cycle.

Finally, it is important to compare the moment arm changes in Figure 8 with the baseline moment arm lengths (see description in Figure 8). MA-EndP lengths do increase for normal walking speed in greater quantities compared to MA-EndP for slow walking speed. However, the changes in MA-EndP length in both speeds do not cause a change in moment arm direction. Also at Mid And HSR, the changes in moment arm do not provide for a shift in moment direction. The baseline MA-EndP, MA-Mid and MA-HSR values are positive which means a backward angular momentum is created.

3.2.2 CoP-CoM distance

To gain better insight into the moment arm, we analyse the horizontal CoP-CoM distance in AP direction for normal and slow walking speed. The effect on the distance after forward and backward perturbation is observable, see Figure 9 and 10. During normal walking, the perturbation magnitudes in forward and backward direction linearly absolute increase CC-EndP (for-

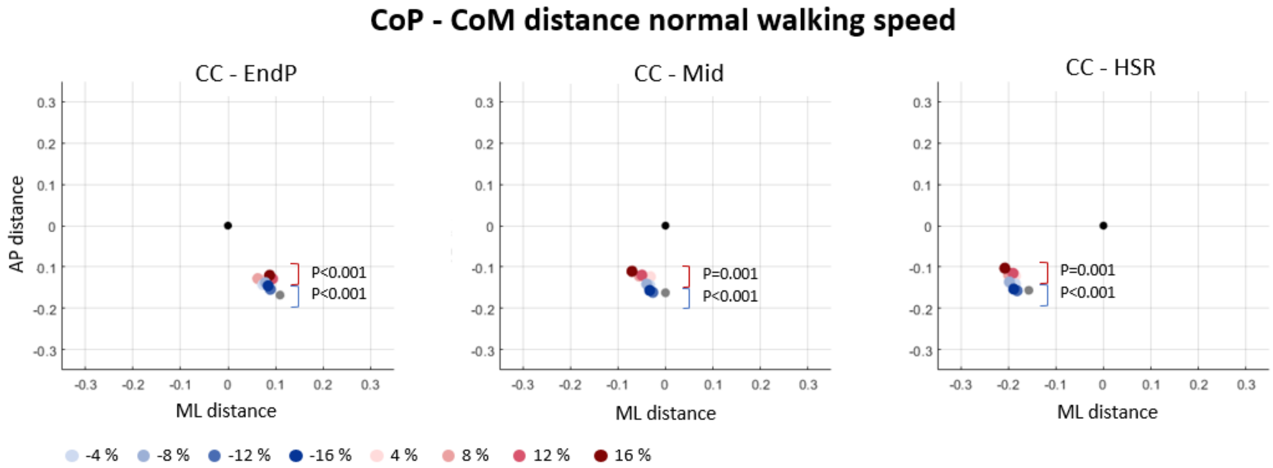

Figure 9: **AP distance between CoP and CoM at EndP, Mid and HSR for normal speed.** The colors of the dots correspond to the legend in Figure 5. The black dot in the middle represents the CoM. The x and y-axis are normalized (using $\sqrt{\text{leg length}}$). The statistical significant results are shown in the figure. Red and blue represent forward and backward perturbations, respectively.

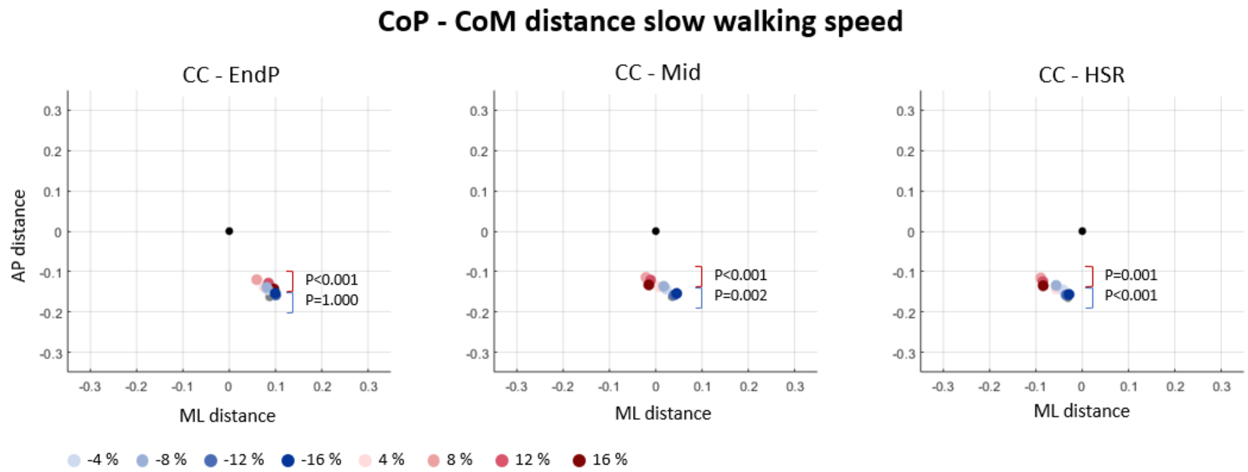

Figure 10: **AP distance between CoP and CoM at EndP, Mid and HSR for slow speed.** The colors of the dots correspond to the legend in Figure 5. The black dot in the middle represents the CoM. The x and y-axis are normalized (using $\sqrt{\text{leg length}}$). The statistical significant results are shown in the figure. Red and blue represent forward and backward perturbations, respectively.

ward perturbation: $p<0.001$, backward perturbation:$p<0.001$), CC-Mid ($p=0.001$,$p<0.001$) and CC-HSR ($p=0.001$,$p<0.001$). However, we observe that CC-EndP shows a less visible change in distance after increasing perturbation magnitude compared to CC-Mid and CC-HSR. However, we see in all three moments that the backward perturbations keep the length close to baseline length while forward perturbations decrease the length. Slow walking shows almost the same results, see Appendix Section 5.1 Figure 13. Here, the perturbation magnitudes significantly affect CC-Mid ($p<0.001$,$p=0.002$) and CC-HSR ($p=0.001$,$p<0.001$) after forward and backward perturbations. Although, CC-EndP shows that increasing backward perturbations did not affect the distance ($p=1.000$). While the forward perturbations did linearly decrease CC-EndP. The statistical test can be explored in Table 4 in Appendix 5.3.

3.2.3 Ground reaction force

At last, we observe the GRF in AP direction.Appendix Section 5.1 Figure 14 shows the GRF in AP direction over the gait cycle. At EndP, an increase (forward perturbations) and decrease (backward perturbations) of GRF change can be seen. Statistical analysis shows that the absolute change in GRF-EndP magnitude is increasing with increasing perturbation magnitude for normal and slow walking and in both directions (forward: $p<0.001$, back-

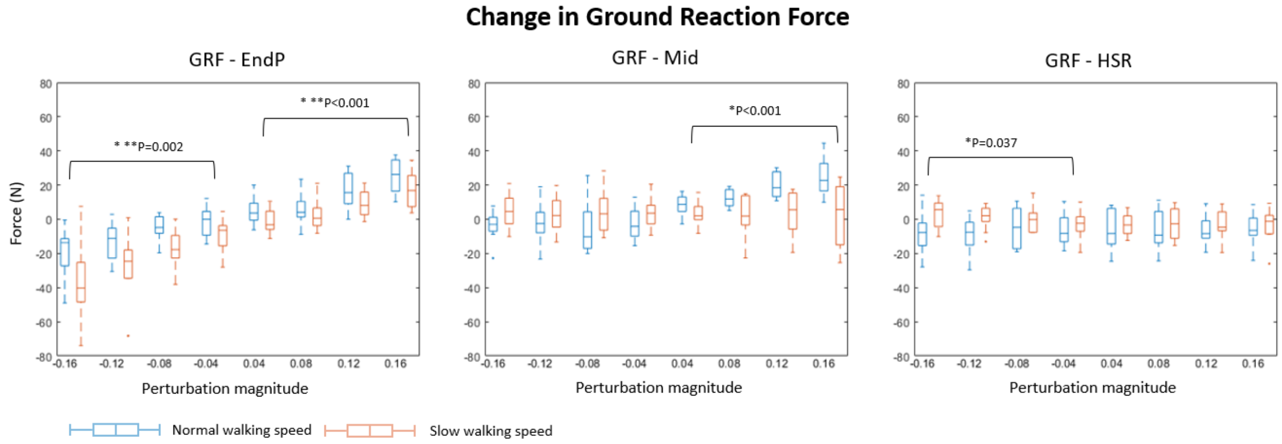

Figure 11: **GRF in AP direction at EndP, Mid and HSR** Boxplots are shown for slow walking speed (orange) and normal walking speed (blue). Negative values represent backward directed GRF and positive values represent forward directed GRF. The baseline value at the specific moment within the gait cycle is subtracted from the perturbation data. Baseline GRF in AP direction values: EndP -34.20 N (normal) and -21.32 N, Mid 0.69 N (normal) and -4.96 N (slow) and HSR 92.79 N (normal) and 31.64 N (slow). A asterisk (*) represent the statistics for normal walking speed and a double asterisk (**) represent the statistics for slow walking speed.

ward: p=0.002). Shortly after, it is visible that backward perturbations do not affect GRF-Mid. Meanwhile, forward perturbations do result in a change in GRF-Mid magnitude ($p<0.001$) but only normal walking speed. GRF-Mid during slow walking speed is not affected by perturbation magnitudes in forward direction but the variability is high. The GRF-HSR shows no increase after increasing perturbation magnitudes in forward direction. This observation is in line with the results of the statistical test. The backward directed perturbation magnitudes had a significant effect on the GRF-HSR for normal walking speed and not for slow walking speed.

The baseline GRF magnitudes are shown in the description of Figure 11. AP directed GRF-EndP baseline value is directed backwards for both walking speeds. The GRF-EndP magnitude at the 16% perturbation are for both speeds almost equal to the baseline value, which results in a GRF magnitude almost equal to zero. Due to negative perturbations, GRF-EndP results in higher backward directed magnitudes. GRF-Mid magnitude is very small for both speeds. However, only forward perturbations during normal walking speed do affect the GRF-Mid significant, the direction remains forward. The GRF-HSR baseline magnitudes are greater compared to GRF-Mid and directed backward in both walking speeds. Minimal changes due to the perturbations cause no GRF-HSR direction shift.

4 Discussion

Ten experiments were conducted with healthy subjects walking on a treadmill receiving upper body and opposite pelvis perturbations. The experiments were performed at two walking speeds: normal (4.4 km/h) and slow speed (1.6 km/h, a typical exoskeleton walking speed). The opposite perturbations resulted in clear changes in CoMv but minimally affected the CoMv. In this study, we focused on the used balance strategy to find balance after the perturbation. We found that there was no significant linear relation between increasing perturbation magnitude and change in moment arm for both perturbation directions and both walking speeds. Statistics showed that increased perturbation magnitudes did affect the CoP-CoM distance in AP direction at the moments EndP, Mid and HSR for both speeds and both perturbation directions. Furthermore, the GRF in AP direction changed significantly due to perturbation magnitude at EndP for both walking speeds.

4.1 Validation of the experiment

In both speeds, the CoMv is minimal affected by perturbations from from TOR to EndP. The duration of one gait cycle during the slow speed is longer while the human reaction time of the remains the same (417 ms [17]). In addition, the duration of the perturbation remains the same what ensures that the subjects has more time from EndP to HSR. This phase is valuable to recover from the perturbation. The overall smaller magnitudes and fluctuations in the CoMv plot at slow speed were likely the result of the lower speed and longer gait cycle duration.

The applied pelvis perturbation is located closer to the CoM compared to the upper body perturbation. Upper body perturbations cause an angular displacement in the legs and trunk, and pelvis perturbations only in the legs. [1] However, we applied upper body and pelvis perturbations but in opposite the direction. The generated angular displacement in legs are in opposite direction. At the same moment, the trunk makes an angular displacement due to only upper body perturbations. The WBAM for slow speed increased more compared to normal walking speed. Bennett et al. found that the walking speed and the WBAM are negatively correlated, which explains the greater impact of the perturbations on slow walking speed [18]. In addition, the stiffness of the joints and muscles increase at higher walking speeds which ultimately affect the WBAM results [19]. A higher joint stiffness minimizes the joint movement [20] and, because the WBAM represents the rotational momentum of all segments, this affects the total WBAM [21].

Focusing on both WBAM and CoMv, we first saw that the forward perturbations give a higher CoMv and an increasing WBAM in forward direction during the perturbation. Secondly, the backward perturbations result in a lower CoMv and backward angular momentum during the perturbation. After the perturbation, the effect of the perturbation direction changes the WBAM in opposite direction than during the perturbation. This shift in WBAM is caused by the balance strategy.

4.2 Balance recovery strategy

A moment arm means that an angular momentum is created. The baseline MA-EndP for both walking speeds is positive which equals a backward angular momentum. After the perturbations in forward direction, the MA-EndP increases and also the magnitude of these backward angular momentum, despite the great variability. However, the backward perturbations decrease the magnitude of angular momenta. This causes, at a perturbation magnitude of 0.16, an angular momentum almost equal to zero for the normal walking speed. MA-Mid is already less affected by perturbations, a backward perturbation is generated due to the positive baseline MA-Mid. Contrary, MA-Mid shows that the backward angular momentum increases for normal walking speed after forward perturbations. Finally, the forward perturbations affect again MA-HSR and therefore also the angular momentum in both walking speeds.

The relation between the moment arm and WBAM can be recognized, observing Figure 7. At EndP, the angular momentum increased in backward or forward direction, dependent on the perturbation direction. After EndP, the body reacted to the perturbation. Here, a small overcompensation in the WBAM occurred in the opposite direction of the WBAM result during the perturbation.

The backward angular momentum was usually generated by a large net joint moment from the hip extensor and a small net joint moment from the knee extensor or flexor by activation of the hamstrings and gluteus maximus [10]. For forward angular momentum, a small net joint moment from the hip extensor or flexor and a large net force moment from the knee extensor are generated by activation of the rectus femoris, the hip flexor and the gluteus maximus [10]. We suggest that the activity of the mentioned muscles for forward and backward angular momentum are largely affected during the perturbation. During walking, biarticular muscles (hamstrings and rectus femoris) stabilize the trunk [22] and are also heavily involved in recovering balance after receiving perturbations on the upper body during standing still. [23] Furthermore, we already discussed that upper body perturbations cause a change in the angular momentum around the hip and legs. These findings combined suggest that the two biarticular muscles are important in balance recovery in this experiment. To gain a better understanding of the effect of the perturbations on muscle activity, studies with EMG measurements need to be carried out. Such a new study could potentially confirm the suggested observations in muscle activation during disbalance. Additional, the exoskeleton needs to understand the intention of the user and needs to provide required assistance. The estimation of joint torques, using muscle activation from EMG, can achieve this goal. Exoskeleton will then assist the users, which enables to perform tasks but also to decrease the muscle effort. [24]

Vlutters el al. [3] found that the CoP-CoM distance in AP direction is linearly related to the horizontal CoMv at HSR and TOL after perturbation. This relation was observed in the case of applying AP pelvis perturbations at TOR. [3]. Although the goal of the present study, was to reach minimal CoMv change, the perturbations did still affect the CoMv a bit. In a response to this (and taking into account the relation found by Vlutters et al.), there is a significant relation between the CoP-CoM distance in AP direction and perturbation magnitudes at EndP, Mid and HSR (Figure 9 and 10). In this study, we only focused on the CoP-CoM distance in AP direction because it affects the moment arm. Although, we observed that the CoP-CoM distance in ML direction is also affected by the perturbations (see Figures 9 and 10). However, no statistical test has been conducted for this variable to test the linear relation with the perturbation magnitudes. In further research, it would be interesting to investigate the effect of perturbing the angular momentum in AP direction on the CoP-CoM distance in ML direction. This would give information about the adjustment in the steps during walking and therefor the possibly occurring disbalance in ML direction.

In general unperturbed walking, the GRF varies within the gait cycle [25]. The increasing backward directed GRF-EndP in AP direction after backward perturbations means that an angular impulse is created in forward direction. This results in an increasing angular momentum. Forward perturbations caused a decreased the backward GRF-EndP. This results in a decreasing angular momentum in forward direction. The backward perturbations provide a greater forward angular momentum than forward perturbations. Observe these angular momentum shift after EndP in Figure 7. These findings indicate that the human reacts directly after the perturbation by adapting the GRF. Changing the angular momentum (by GRF) counteracts the minimal affected CoMv, which brings the perturbed CoMv near the baseline CoMv. Besides, this also explains the change in angular momentum since the GRF affects the angular acceleration. The moment between EndP and HSR points out that GRF after forward perturbations linearly increases with perturbation magnitude during normal speed, causing a backward angular momentum. At this moment, the WBAM after the positive perturbations is, because of this change in GRF, closer to the baseline WBAM. The angular momentum at HSR is minimally affected by perturbation magnitude. A small but significant trend is visible at the backward perturbation for slow walking. This indicates that the body is still recovering from the disbalance.

Summarizing, we found that a perturbed angular momentum affects the WBAM. During the perturbation, the GRF AP direction is affected causing an increase or decrease in angular momentum. After the perturbation, the AP directed GRF is in opposite direction than the GRF during the perturbation which created an angular momentum in opposite direction. This results in an angular momentum closer to the baseline, giving that the body recovers from the disbalance.

The differences between the two walking speeds in the three moments can, firstly, be related to the reaction time [17]. The duration of the gait cycle is larger in slow walking, which leads to more time to think of how how to adapt to the disbalance. This could be the cause of the longer-lasting effect of the perturbation for normal walking speed in the moment arm and in the GRF compared to slow walking speed (Figures 8 and 11). Secondly, the stiffness of joints depend on the muscle activation, the joint angle and the displacement amplitude of the joint [26]. During normal walking speed, a higher GRF magnitude can be observed (see baseline GRF magnitudes in the description of Figure 11), induced by larger muscle activation and therefore a greater joint stiffness. However, we observe between the two walking speeds no remarkable differences in GRF change due to perturbations. Besides the GRF, the WBAM also differs between the two walking speeds. The higher absolute WBAM and the smaller GRFs during slow walking compared to normal walking speed, show that the stiffness of joints are smaller in slow walking speed. In the current study, we focused on the balance strategy after perturbing the angular momentum during two walking speeds. However, the goal was not to statistically compare the balance strategies between the two walking speeds. In further research, this statistical analysis would provide more insight into the differences in recovering from a perturbed angular momentum between normal and slow walking speed.

The backward and forward perturbation affect the balance strategy in different way. Looking back at the WBAM in Figure 7, the backward perturbations affect the WBAM more from the end of perturbation to HSR during both walking speeds compared to forward perturbations. It is known that after backward perturbations, the risk of falling is higher than after forward perturbations. [10] Backward instability is partly caused by the limited ability to adapt the CoP in the posterior direction compared to the anterior direction. [27] This results in favouring the stepping strategy instead of the ankle and hip strategy (which are less energy-consuming). [28] This instability after backward perturbations is reflected in the WBAM. Furthermore, the backward and forward falling direction activate multi joints in opposite directions. A forward movement uses ankle plantar flexor, knee flexor and hip extensor net joint moments to neutralize the disbalance. The backward movements finds balance using the ankle plantar flexor, knee extension and hip flexion net joint moments. [10] The differences in hip and knee movement indicate that the activation of muscles are different for forward and backward falling. [10] Again, these findings can be further elaborated with EMG measurements. It is important that the human-like controller of the exoskeleton must adapts its assistance to perturbation direction. [29]

Ultimately, the goal is to implement these balance strategies in the human-like controller of the exoskeleton. The exoskeleton assists the patient as needed. This means that the exoskeleton has to detect in real time the moment of balance loss. After this moment is detected, the exoskeleton will assist the patient with tasks. Estimation of CoM and angular momentum in the control of the exoskeleton is important. [30] This study investigates only the perturbed angular momentum. Studying the balance loss after perturbing the angular momentum will help the exoskeleton to provide appropriate assistance. [29] Future studies, focused on the balance strategy after perturbing the angular momentum, could consider to evaluate EMG measurement of the muscles which are involved in finding balance.

4.3 Limitations

The present study has several limitations. During the experiments, the subjects needed to become accustomed to the treadmill and walking speeds. At the beginning of the experiment, the subjects seemed to walk with stiffer arms compared to normal walking over ground and also compared to the last trials of the experiment. This may affect the motion of the body after perturbations, as stiffness affects joint movements. [21]. This limitation also affects the measured displacement of segments (CoM), rotations of the body (WBAM) and ground reaction forces (GRF). Allowing arm movements during the experiments is related to the envisioned end goals, as humans walking in exoskeletons could also use arm movement. Therefore, knowledge of the balance strategy of the human with arm movement is relevant. During the experiments of the current study, perturbations are given at TOR, and the results above are only relevant for perturbations at this specific moment. However, we expect that applying the same perturbation at TOL would result in equal balance strategies under the assumption of a symmetric gait pattern. Nowadays, perturbing the angular momentum is not investigated at other moments within the gait cycle. Performing these perturbation at different moments would lead to more knowledge about the balance strategy.

4.4 Conclusion

Simultaneous perturbations on the upper body and pelvis but in opposite direction caused an affected WBAM and minimal change in CoMv. We analysed the moment arm, the CoP-CoM distance in AP direction and the GRF in AP direction. The perturbations caused a greater backward angular momentum during backward perturbation and greater forward angular momentum during forward perturbations. After the perturbation, the GRF (AP directed) changes its direction in the opposite direction. This new opposite created angular momentum solves the disbalance in WBAM. In addition, the disbalance is mainly solve in the first half gait cycle. Future studies are necessary to investigate which muscles are involved in the balance strategy. A better understanding of the balance strategies may contribute to a better human-like controller for the exoskeleton.

Table 2: Glossary

Abbreviation	Meaning
AP	Anteroposterior
BoS	Base of Support: The area on the floor between and under the contact points of the person with the ground
CC	CoP-CoM distance
CoM	Centre of Mass: the virtual mass point of a human
CoMv	Centre of Mass velocity.
CoP	Centre of Pressure: point of application of the GRF
EndP	End of the perturbation
GRF	External force exerted by the ground on the human body
MA	Moment arm
Mid	Moment in gait cycle between EndP and HSR
ML	Mediolateral
XCoM	Extrapolated centre of mass. Indicator for stable walking.
WBAM	Whole Body Angular Momentum: the angular momentum around the CoM

References

[1] S. Rietdyk, A. E. Patla, D. A. Winter, M. G. Ishac, and C. E. Little. Balance recovery from medio-lateral perturbations of the upper body during standing. In *Journal of Biomechanics*, volume 32, pages 1149–1158. Elsevier Science Ltd, nov 1999.

[2] Maud van den Bogaart, Sjoerd M. Bruijn, Jaap H. van Dieën, and Pieter Meyns. The effect of anteroposterior perturbations on the control of the center of mass during treadmill walking. *Journal of Biomechanics*, 103, apr 2020.

[3] M. Vlutters, E. H.F. Van Asseldonk, and H. Van Der Kooij. Center of mass velocity-based predictions in balance recovery following pelvis perturbations during human walking. *Journal of Experimental Biology*, 219(10):1514–1523, may 2016.

[4] A. L. Hof, M. G.J. Gazendam, and W. E. Sinke. The condition for dynamic stability. *Journal of Biomechanics*, 38(1):1–8, jan 2005.

[5] At L. Hof. The 'extrapolated center of mass' concept suggests a simple control of balance in walking. *Human Movement Science*, 27(1):112–125, feb 2008.

[6] Awais Yasin, Qiang Huang, Qian Xu, and M. Saad Sultan. Humanoid robot push recovery through foot placement. In *2012 IEEE International Conference on Mechatronics and Automation, ICMA 2012*, pages 59–63, 2012.

[7] Aftab E. Patla. Strategies for Dynamic Stability During Adaptive Human Locomotion, mar 2003.

[8] Forough Madehkhaksar, Jochen Klenk, Kim Sczuka, Katharina Gordt, Itshak Melzer, and Michael Schwenk. The effects of unexpected mechanical perturbations during treadmill walking on spatiotemporal gait parameters, and the dynamic stability measures by which to quantify postural response. *PLoS ONE*, 13(4), apr 2018.

[9] Riley C. Sheehan, Eduardo J. Beltran, Jonathan B. Dingwell, and Jason M. Wilken. Mediolateral angular momentum changes in persons with amputation during perturbed walking. *Gait and Posture*, 41(3):795–800, mar 2015.

[10] Witaya Mathiyakom and Jill L Mcnitt-Gray. Regulation of angular impulse during fall recovery. *Journal of Rehabilitation Research Development*, 45(8):1237–1248, 2008.

[11] Kreg G Gruben and Wendy L Boehm. Ankle torque control that shifts the center of pressure from heel to toe contributes non-zero sagittal plane angular momentum during human walking.

[12] Jonathan B. Dingwell and Laura C. Marin. Kinematic variability and local dynamic stability of upper body motions when walking at different speeds. *Journal of Biomechanics*, 39(3):444–452, jan 2006.

[13] Amy R. Wu, Cole S. Simpson, Edwin H. F. van Asseldonk, Herman van der Kooij, and Auke J. Ijspeert. Mechanics of very slow human walking. *Scientific Reports 2019 9:1*, 9(1):1–10, dec 2019.

[14] T. Bhatt, J. D. Wening, and Y. C. Pai. Influence of gait speed on stability: recovery from anterior slips and compensatory stepping. *Gait Posture*, 21(2):146–156, feb 2005.

[15] At L. Hof. Scaling gait data to body size, may 1996.

[16] Hugh Herr and Marko Popovic. Angular momentum in human walking. *Journal of Experimental Biology*, 211(4):467–481, feb 2008.

[17] Stefan Delmas, Agostina Casamento-Moran, Seoung Hoon Park, Basma Yacoubi, and Evangelos A. Christou. 120(4):2059–2065, oct 2018.

[18] Bradford C Bennett, Shawn D Russell, Pradip Sheth, and Mark F Abel. Angular momentum of walking at different speeds Human Movement Science. *Human Movement Science*, 29:114–124, 2010.

[19] Arampatzis A, Schade F, Walsh M, and Brüggemann GP. Influence of leg stiffness and its effect on myodynamic jumping performance. *Journal of electromyography and*

kinesiology : official journal of the International Society of Electrophysiological Kinesiology, 11(5):355–364, 2001.

[20] McHugh MP and Hogan DE. Effect of knee flexion angle on active joint stiffness. *Acta physiologica Scandinavica*, 180(3):249–254, mar 2004.

[21] Jenny A. Kent, Joel H. Sommerfeld, and Nicholas Stergiou. Changes in human walking dynamics induced by uneven terrain are reduced with ongoing exposure, but a higher variability persists. *Scientific Reports 2019 9:1*, 9(1):1–9, nov 2019.

[22] Prilutsky BI, Gregor RJ, and Ryan MM. Coordination of two-joint rectus femoris and hamstrings during the swing phase of human walking and running. *Experimental brain research*, 120(4):479–486, 1998.

[23] Christian Schumacher, Andrew Berry, Daniel Lemus, Christian Rode, André Seyfarth, and Heike Vallery. Biarticular muscles are most responsive to upper-body pitch perturbations in human standing. *Scientific Reports*, 9(1), dec 2019.

[24] Tommaso Lenzi, Stefano Marco Maria De Rossi, Nicola Vitiello, and Maria Chiara Carrozza. Intention-based EMG control for powered exoskeletons. *IEEE Transactions on Biomedical Engineering*, 59(8):2180–2190, 2012.

[25] Hadar Shaulian, Deborah Solomonow-Avnon, Amir Herman, Nimrod Rozen, Amir Haim, and Alon Wolf. The effect of center of pressure alteration on the ground reaction force during gait: A statistical model. *Gait and Posture*, 66:107–113, oct 2018.

[26] Schouten AC, Boonstra TA, Nieuwenhuis F, Campfens SF, and van der Kooij H. A bilateral ankle manipulator to investigate human balance control. *IEEE transactions on neural systems and rehabilitation engineering : a publication of the IEEE Engineering in Medicine and Biology Society*, 19(6):660–669, dec 2011.

[27] Winter DA, Prince F, Frank JS, Powell C, and Zabjek KF. Unified theory regarding A/P and M/L balance in quiet stance. *Journal of neurophysiology*, 75(6):2334–2343, 1996.

[28] William E. McIlroy and Brian E. Maki. Age-related Changes in Compensatory Stepping in Response to Unpredictable Perturbations. *The Journals of Gerontology: Series A*, 51A(6):M289–M296, nov 1996.

[29] Fusheng Zha, Wentao Sheng, Wei Guo, Shiyin Qiu, Xin Wang, and Fei Chen. The exoskeleton balance assistance control strategy based on single step balance assessment. *Applied Sciences (Switzerland)*, 9(5), 2019.

[30] François Bailly, Justin Carpentier, Mehdi Benallegue, Bruno Watier, Philippe Souères, Philippe Souères Estimat-, and PhilippeSoù Eres. Estimating the Center of Mass and the Angular Momentum Derivative for Legged Locomotion-A recursive approach. *IEEE Robotics and Automation Letters*, 2019(4):4155–4162.

5 Appendix

5.1 Moment arm, GRF and CoP-Com distance over the gait cycle

Explanation about the Figures 12, 14 and 13: Solely the left foot data is graphed because we analyse only the first half gait cycle in this study. At HSR, the right foot is just on the ground what gives inaccurate values. This makes the left foot more valuable to use for the analysis at HSR. In addition, the two double support phases, HSR-TOL and HSL-TOR, represent only left foot values.

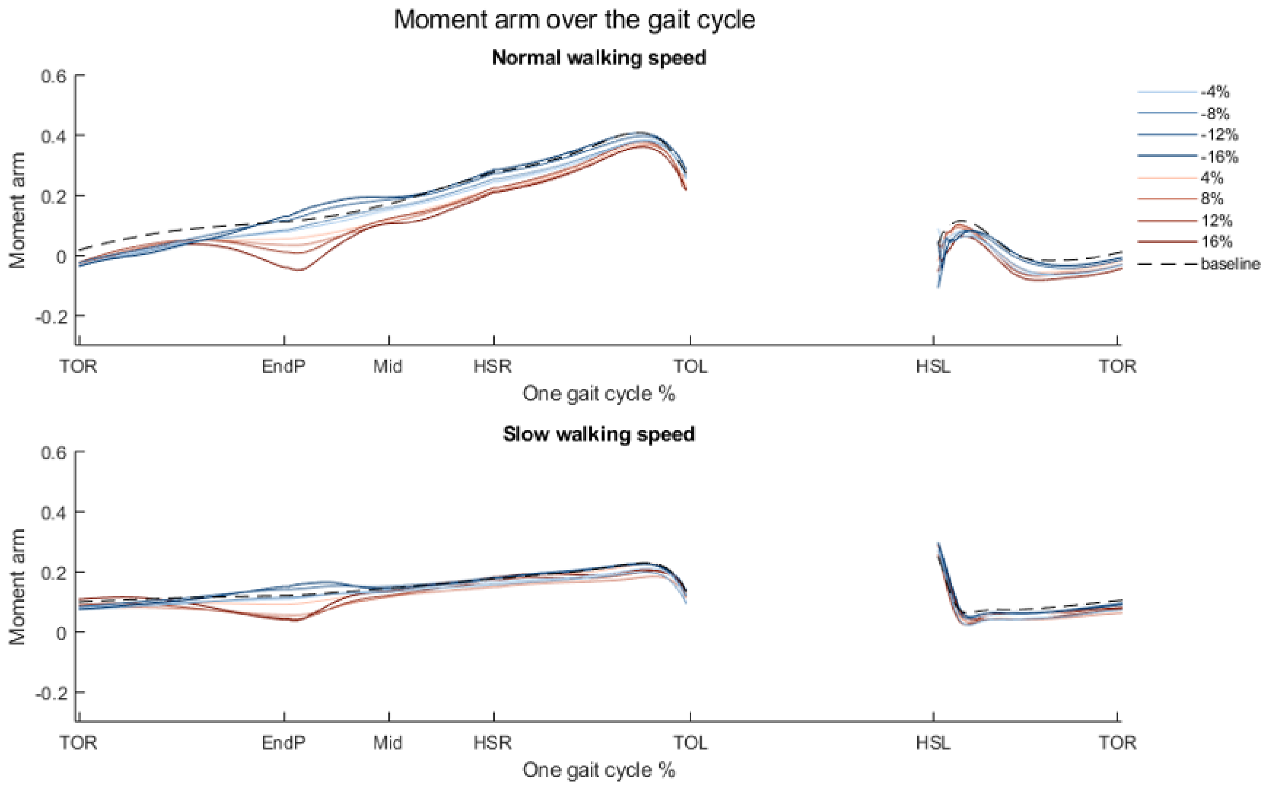

Figure 12: **Moment arm over the gait cycle.** Only the values of the left foot are used. See Appendix 5.1 for a better explanation.

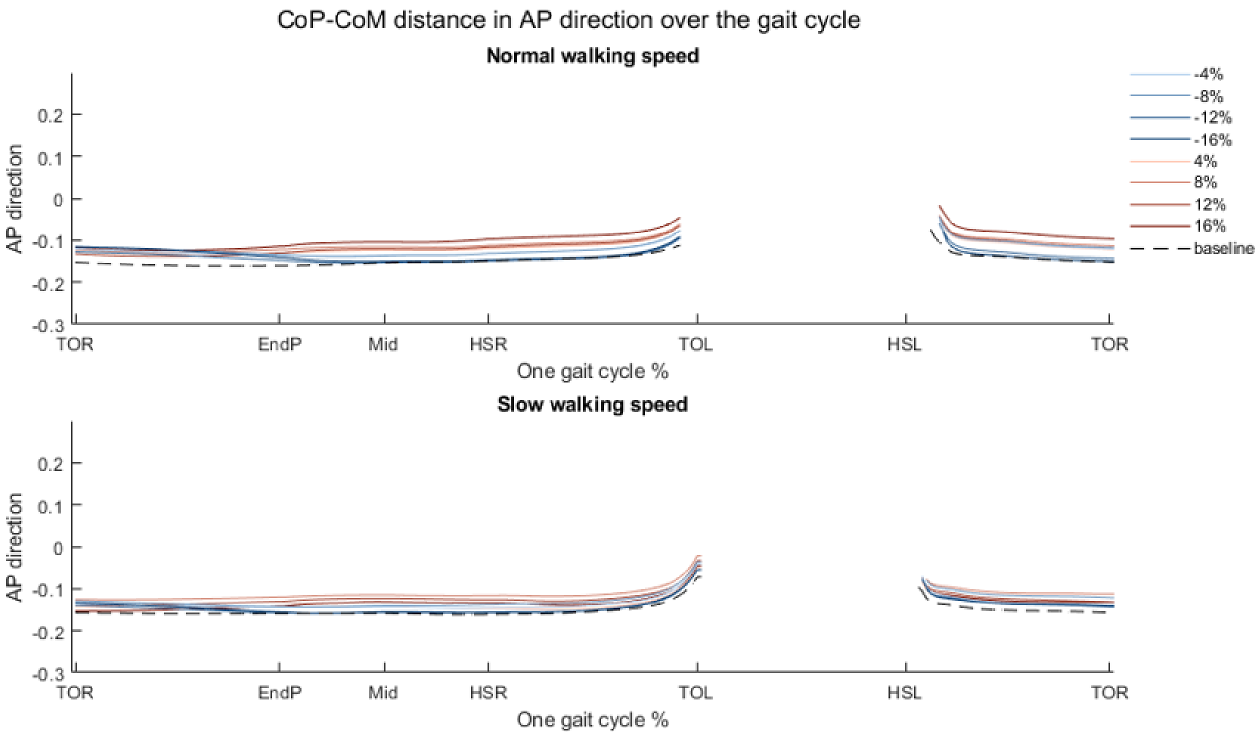

Figure 13: **CoP-CoM distance in AP direction over the gait cycle.** Only the values of the left foot are used. See Appendix 5.1 for a better explanation.

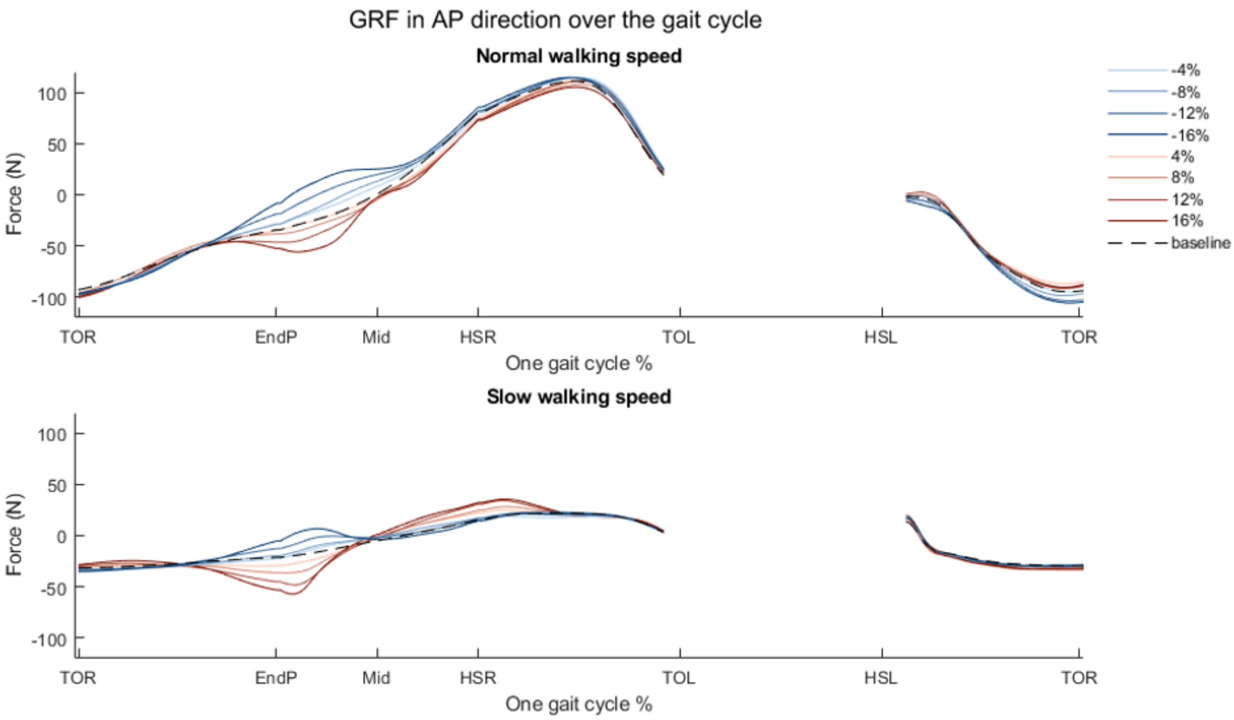

Figure 14: **GRF in AP direction over the gait cycle.** Only the values of the left foot are used. See Appendix 5.1 for a better explanation.

5.2 Mixed linear model moment arm

Table 3: **Mixed linear model statistical analysis of the moment arm.** The moments EndP, Mid and HSR during both walking speed are tested. The perturbation magnitudes are separated into two groups: the positive and negative perturbations, as explained in the statistics section.

	Estimate ± Std. Error	*t(df)*	*p (Sig.)*
EndP, normal			
Negative	-2.215 ± 1.779	-1.25(43)	0.220
Positive	1.770 ± 1.377	1.29(35)	0.207
EndP, slow			
Negative	6.038 ± 1.879	3.21(35)	0.003
Positive	-1.601 ± 1.286	-1.25(12.73)	0.236
Between EndP and HSR, normal			
Negative	0.991 ± 2.060	0.48(10.97)	0.640
Positive	-0.507 ± 1.954	-0.26(9.89)	0.801
Between EndP and HSR, slow			
Negative	-1.605 ± 1.864	-0.86(14.78)	0.403
Positive	2.108 ± 1.847	1.14(34.77)	0.262
HSR, normal			
Negative	0.931 ± 1.401	0.67(8.56)	0.523
Positive	-0.946 ± 1.764	-0.54(8.24)	0.606
HSR, slow			
Negative	-2.149 ± 1.229	-1.75(9.50)	0.112
Positive	-0.179 ± 0.971	-0.19(9.26)	0.857

5.3 Mixed linear model CoP-CoM

Table 4: **Mixed linear model statistical analysis of the CoP-CoM distance.** The moments EndP, Mid and HSR during both walking speed are tested. The perturbation magnitudes are separated into two groups: the positive and negative perturbations, as explained in the statistics section.

	Estimate ± Std. Error	*t(df)*	*p (Sig.)*
EndP, normal			
AP direction: negative	-0.349 ± 0.071	-4.89(33.41)	<0.001
AP direction: positive	0.292 ± 0.077	3.82(41.00)	<0.001
EndP, slow			
AP direction: negative	-0.421 ± 0.097	-4.34(0.00)	1.000
AP direction: positive	0.341 ± 0.083	4.12(33.05)	<0.001
Mid, normal			
AP direction: negative	-0.337 ± 0.067	-5.01(33.50)	<0.001
AP direction: positive	0.246 ± 0.065	3.80(33.45)	0.001
Mid, slow			
AP direction: negative	-0.336 ± 0.100	-3.35(35.00)	0.002
AP direction: positive	-0.358 ± 0.084	-4.28(195249.69)	<0.001
HSR, normal			
AP direction: negative	-0.275 ± 0.059	-4.68(33.35)	<0.001
AP direction: positive	0.216 ± 0.058	3.73(33.37)	0.001
HSR, slow			
AP direction: negative	-0.362 ± 0.077	-4.70(33.48)	<0.001
AP direction: positive	0.293 ± 0.077	3.80(33.18)	0.001

5.4 Mixed linear model GRF

Table 5: **Mixed linear model statistical analysis of the GRF in AP direction.** The moments EndP, Mid and HSR during both walking speed are tested. The perturbation magnitudes are separated into two groups: the positive and negative perturbations, as explained in the statistics section.

	Estimate ± Std. Error	*t(df)*	*p (Sig.)*
EndP, normal			
AP direction: negative	126.796 ± 28.449	4.46(8.78)	0.002
AP direction: positive	156.45 ± 18.993	8.24(8.85)	<0.001
EndP, slow			
AP direction: negative	220.612 ± 49.65	4.44(8.11)	0.002
AP direction: positive	113.81 ± 19.68	5.78(8.89)	<0.001
Between EndP and HSR, normal			
AP direction: negative	19.981 ± 20.032	0.99(9.80)	0.343
AP direction: positive	152.503 ± 25.389	6.01(8.04)	<0.001
Between EndP and HSR, slow			
AP direction: negative	-28.461 ± 22.189	-1.28(8.68)	0.233
AP direction: positive	11.480 ± 41.84	0.28(8.04)	0.789
HSR, normal			
AP direction: negative	43.908 ± 17.874	2.46(8.77)	0.037
AP direction: positive	-21.623 ± 12.990	-1.67(35.44)	0.105
HSR, slow			
AP direction: negative	-29.150 ± 14.235	-2.35(8.71)	0.072
AP direction: positive	-17.482 ± 9.387	-1.86(7.93)	0.100